# 4 Sample Preparation

Having studied the theory and experimental setup of the light scattering method in the preceding chapters, let us now consider how light scattering samples are prepared in practice.

The sample cells suitable for the experiment have to be chosen according to experimental conditions, such as light scattering detected offline or in combination with a fractionation technique, and sample parameters (amount, temperature, pressure, etc.). If light scattering detectors are used in combination with chromatography or field flow fractionation, special commercially available flow cells have to be used. For most discontinuous measurements of aqueous or nonaqueous solutions of the scattering nanoparticles or polymers, cylindrical quartz glass cuvettes with an outer diameter between 1 cm and 3 cm are useful (see Chap. 6 for commercial provider). For high temperature samples like nanoparticles dispersed in a polymer melt, special sample cells, often home-built, are needed. In this chapter about the preparation of light scattering samples, I will restrict myself to the most common experimental practice of light scattering: characterization of particles in solution at room temperature.

The sample parameters summarized in Table 4.1 are needed for quantitative light scattering data analysis and have to be determined either experimentally or to be looked-up in standard manuals like the well-known "Handbook of Physical Chemistry".

Note that there is a difference in the parameters needed for static light scattering or dynamic light scattering. The parameters listed in Table 4.1 follow from the key equations for static (Eqs. 1.9 and 1.21), Zimm analysis) and dynamic light

**Table 4.1.** Sample parameters needed for data evaluation in light scattering experiments

| Parameter | Static light scattering | Dynamic light scattering |
|---|---|---|
| Solvent viscosity $\eta$ | No | Yes |
| Solvent refractive index $n_D$ | Yes | Yes |
| Sample concentration in g/L | Yes | No |
| Sample temperature | No | Yes |
| Refractive index increment $dn_D/dc$ | Yes | No |

scattering (Eq. 1.47, Stokes–Einstein–equation), respectively. The refractive index of the solvent is needed in all cases since it determines the magnitude of the scattering vector $q$ according to Eq. 1.14. Whereas pure solvent quantities as viscosity $\eta$ or refractive index $n_D$ can be looked up in tables, for instance in the Handbook of Physical Chemistry, the refractive index increment $dn_D/dc$ often has to be measured, for example, if the solute scattering particles consist of non-standard chemicals or mixed chemical components. For this purpose, commercial interferometers with sufficient accuracy are available from most companies who also provide commercial light scattering setups (see Chap. 3). In Chap. 6.3 of this book, solvent characteristics $\eta$ and $n_D$ as well as refractive index increments $dn_D/dc$ for the most common solvents and polymer-solvent pairs used in light scattering experiments are presented.

## 4.1 Sample Concentration and Interparticle Interactions

Since we are interested in single particle characterization, the samples should be as dilute as possible to suppress interparticle interactions, which may create contributions from interparticle interferences (structure factor, see Chap. 1) to the angular dependence of the detected scattered intensity, and therefore spoil the form factor analysis in the static light scattering experiment. Also, the Stokes–Einstein–equation (Eq. 1.47) in this case is no longer valid, and diffusion coefficients determined by dynamic light scattering yield wrong hydrodynamic radii. On the other hand, the concentration of scattering particles within solution has to be large enough to create sufficient scattered intensity at all scattering angles of interest (typically in the range 30° to 150°). Here, the reader should remember that the scattered intensity depends on the following parameters: (i) mass or size of the scattering particles, which unfortunately cannot be adjusted to experimental needs; (ii) solute particle concentration, which should be as small as possible; and (iii) refractive index difference of solvent and solute particles or, more accurate, refractive index increment $dn_D/dc$, which can be adjusted by choosing an appropriate solvent. Importantly, one has to keep in mind that specific solvent-solute interactions, like the formation of aggregates or micelles or even particle disintegration, also have to be avoided.

Whereas nonpolar organic samples usually are not critical up to solute concentrations in the range 1 g/L to 10 g/L, charged systems, also called polyelectrolytes, are more difficult to handle both in water and in organic solvents due to the long-range Coulomb interactions between the scattering solute particles. These interactions may influence the experimental results both in static and dynamic light scattering measurement even at seemingly low particle concentrations <1 g/L. One common solution to this problem is to screen the disturbing Coulomb interactions by adding salt, while not changing the refractive index too much: typical salt concentrations vary from 10e-5 mol/L to 10e-2 mol/L depending on the sample concentration. For charged linear polymer chains, it is commonly agreed that at

a molar concentration ratio c(monomer)/c(salt) <1 Coulomb interactions become negligible (see ref. [4.1] ). In case of branched polyelectrolytes, for example copolymer micelles with charged corona chains in aqueous solution, Förster et al. [4.2] have encountered in their light scattering experiments no specific polyelectrolyte effects (like a structure factor peak in static light scattering or a second slow relaxation process ("slow mode") in dynamic light scattering) at c(monomer) /c(salt) <25. This leads to the conclusion that for branched charged polymers a much lower amount of added salt is sufficient to screen the Coulomb interactions than in case of linear polyelectrolyte chains, a consequence of the lower effective charge per monomer in case of dense polyelectrolyte systems like micelles, brushes, colloidal spheres, dendrimers, and so on. For a detailed review about light scattering studies of polyelectrolytes as well as the properties of polyelectrolytes in solution in general, the interested reader should consult the comprehensive nice review article by Förster and Schmidt about "polyelectrolytes in solution" [4.1].

The added salts most frequently used to screen charge interactions in aqueous solution are KBr, NaBr, or NaCl, whereas for organic solvents either LiBr [tetrahydrofurane (THF), dimethylformamide (DMF), dimethylacetamide (DMA)], or $NBut_4Br$ [chloroform ($CHCl_3$), dichloromethylene ($CH_2Cl_2$), o-dichlorobenzene] are recommended. Figure 4.1 shows the effect of added salt (here: 1.02 g/L LiBr and 0.872 g/L hyperbranched polyelectrolyte dissolved in DMF) on static light scattering results.

Whereas in case of no added salt a structure factor peak is clearly visible in the average scattered intensity, this peak disappears if LiBr is added, and the linear slope of $Kc/R$ plotted versus $q^2$, expected for static light scattering in the Zimm regime, is obtained. Figure 4.1 also shows a Zimm plot of the same sample at five different concentrations, from which weight average molar mass and z-average radius of gyration of the polyelectrolyte nanoparticles could be determined.

The effect of a structure factor, caused by Coulomb interactions between charged polyelectrolyte chains, on both dynamic and static light scattering, has been explored in detail by Förster et al. [4.3]: for salt-free aqueous solutions of quaternized poly(2-vinylpyridine), the reciprocal static scattered intensity plotted vs. $q^2$ showed a negative slope at low polymer concentration, which according to the Zimm equation (Eq. 1.21) would correspond to a negative radius of gyration $R_g$. Interestingly, if the polymer concentration was increased, Förster et al. obtained a straight line as expected for a Zimm plot of small noninteracting polymer coils. In this case, however, the extracted radius of gyration was larger than even expected for a rigid rod. If salt (KBr) was added to a salt-free highly diluted (c = 0.3 g/L) polyelectrolyte solution, the negative slope of the inverse scattered intensity versus $q^2$ changed from negative to positive as expected. Importantly, the radius of gyration decreased if the added salt concentration was increased from 0.01 mol/L to 0.1 mol/L, which indicates a collapse of the polyelectrolyte coil at high added salt concentration. The studies by Förster et al. illustrate an important aspect of the static light scattering characterization of polyelectrolytes not discussed so far: not only does the occurrence of a structure factor peak interfere with the analysis of the particle form factor. Importantly,

there is also the possibility of a change of the particle structure itself depending on the concentration of salt, which has to be added to screen the interparticle interactions.

If in experimental practice one is not sure about the appropriate sample and salt concentrations, it is recommended to conduct the light scattering measurements at

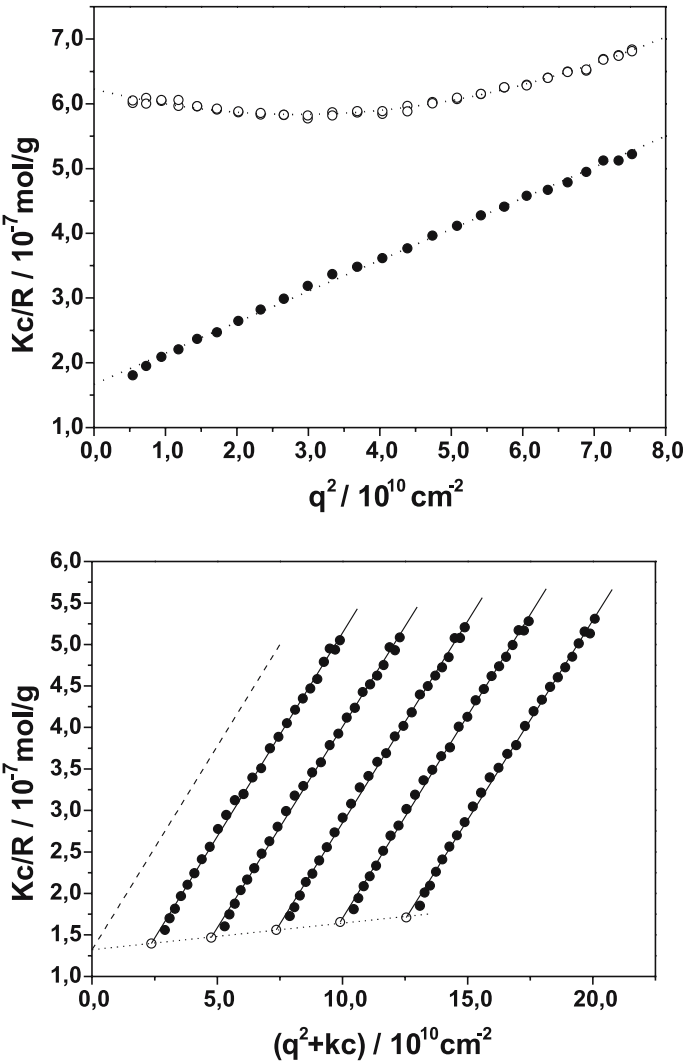


**Fig. 4.1.** Static light scattering results for charged supramolecular nanoparticles without (*open circles*) and with added salt (*filled circles*) (*top*), and Zimm plot for SLS from the noninteracting nanoparticles with added LiBr at various particle concentrations.
[unpublished results, courtesy Dr. K. Fischer and Prof. A.D. Schlüter (Mainz, Zürich 2006)].

given salt concentration and various sample concentrations, covering at least one order of magnitude in the regime 0.1 <c(monomer)/c(salt) <1. If, in a dynamic light scattering experiment, the experimentally determined hydrodynamic radius of the scattering solute particles does not change with concentration, one can be fairly confident that the chosen concentration range is appropriate. For static light scattering, on the other hand, the shape of the scattered intensity plotted versus scattering vector $q$ should not depend on concentration to ensure that only the particle form factor is measured and no unwanted side effects, like structure factor contributions, are detected (see Fig. 4.1).

The addition of added salt has an important consequence on the data analysis of the static light scattering experiment. Whereas for noncharged samples the refractive index increment $dn_D/dc$ is needed to determine the scattering contrast, for charged particles also concentration fluctuations of the small ions (added salt and counter ions) contribute to the scattered intensity. As was shown by Vrij and Overbeek nearly 50 years ago, in this case the refractive index increments have to be measured under conditions defined by the Donnan equilibrium, that is not at constant salt concentration but at constant chemical potential [4.4].

Before we continue with the consequences of the addition of salt for the interpretation of static light scattering measurements, let us briefly review the Donnan equilibrium shown in Fig. 4.2.

As shown, the reader should imagine two chambers separated by a semipermeable membrane. Initially or before the Donnan equilibrium is established, the left chamber shall contain an aqueous solution of negatively charged nanoparticles and positive counterions only, whereas the right chamber contains an aqueous salt solution. For convenience, identical counter ions and cations of the salt have been chosen. The membrane is only permeable for the small ions ($K^+$, $Cl^-$), but impermeable to the larger negatively charged nanoparticles. To establish the electrochemical equilibrium, $Cl^-$ ions will start to flow through the membrane from the right chamber into the left chamber, leading to an electric membrane

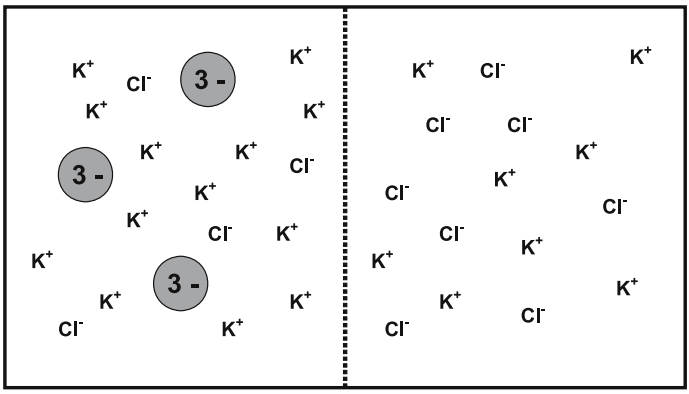


**Fig. 4.2.** Donnan equilibrium for charged nanoparticles in solution with added salt

potential attracting also the $K^+$ ions from right to left. The equilibrium situation illustrated in Fig. 4.2 is established, if the electrochemical potential of all small ions has become equal in the left and right chamber, respectively.

This equilibrium importantly corresponds to a difference in salt concentration between the two chambers: the left chamber containing the charged nanoparticles contains a lower amount of added salt than present in the right chamber, and a small electric membrane potential has built up between the two chambers. The difference in small ion concentrations also causes an osmotic pressure, leading to a solvent flow from the right chamber to the left chamber in case the chamber walls are not solid.

Coming back to static light scattering of charged particles in a solution containing added salt, Vrij and Overbeek showed that the apparent molar mass $M_1{}^*$ determined by Zimm analysis, using the concentration-dependent refractive index increments at constant salt concentration, is given as:

$$M_1{}^* = M_1 \cdot \left[ 1 + \frac{\left(dn_D/dc_2\right)_{c_1}}{\left(dn_D/dc_1\right)_{c_2}} \left( \frac{dc_2}{dc_1} \right)_{\mu_2} \right]^2 \tag{4.1.}$$

Component 1 are the charged nanoparticles, component 2 is the added salt, and $M_1$ is the true molar mass of the nanoparticles. Note that the counter ions because of their usually small number (compared to the added salt ions) obviously are ignored in Eq. 4.1. The most obvious contribution to the term $\left(dc_2/dc_1\right)_{\mu_2}$ originates from the electrical double layer around the polyelectrolyte particles, which corresponds to a seat of negative adsorption of the small ions of the added salt. In simpler terms, the concentration of added salt will be smaller in the immediate vicinity of the nanoparticles than the solution average. Vrij and Overbeek tested their theoretical concept with turbidity measurements, which can be considered as a technically primitive version of modern static light scattering, for solutions of polymethacrylic acid (PMA) polyelectrolyte chains in aqueous HCl and in various salt solutions. Refractive index increments $\left(dn_D/dc_2\right)_{c_1=0}$ and $\left(dn_D/dc_1\right)_{c_2}$ were determined with a Rayleigh interferometer (fabricated by Zeiss). To measure the refractive index increment $\left(dn_D/dc_1\right)_{\mu_2}$, the solutions were dialyzed against a larger reservoir containing an aqueous salt solution with the same salt concentration $c_2$ (as used for the measurement of $\left(dn_D/dc_1\right)_{c_2}$) for 24 h, so the Donnan equilibrium was established. For typical salt species like NaCl or NaBr and salt concentrations $c_2 = 0.1$ Mol/L, the difference between $\left(dn_D/dc_1\right)_{c_2}$ and $\left(dn_D/dc_1\right)_{\mu_2}$ was the order of 10%. This leads to a corresponding difference in apparent molar mass $M_1{}^*$ and true particle molar mass $M_1$, with $M_1 > M_1{}^*$. Since the scattered intensity depends on $\left(dn_D/dc_1\right)^2$ (see Eq. 1.10), the effect of the small ion concentration fluctuations on the molar mass detected by static light scattering is even much larger than 10%. We conclude therefore that in experimental practice the Donnan equilibrium should be established by dialysis of the light scattering sample without added salt versus a large reservoir of a pure salt solution

(with concentration $c_2$). The large size of the salt solution reservoir, compared to the sample volume, guarantees that the salt concentration in the reservoir remains nearly constant while the equilibrium is established, since only a very small amount of salt will diffuse into the sample volume. Both refractive index increments and average scattered intensities have to be determined under these membrane equilibrium conditions to accurately determine the true particle molar mass $M_1$.

In case the static light scattering measurements were performed for aqueous sample solutions with different types of added salt, Eq. 4.1 provides the basis for determination of the true molar mass of the polyelectrolyte particles by conventional static light scattering, meaning even in case no dialysis is used to establish the Donnan equilibrium for measurement of $\left(dn_D/dc_1\right)_{\mu_2}$. By plotting $\sqrt{M_1}^*$ versus $M_2 \cdot \left(dn_D/dc_2\right)_{c_1=0}$, $M_1$ is obtained as the intercept with the axis $M_2 \cdot \left(dn_D/dc_2\right)_{c_1=0} = 0$.

## 4.2 Sample Purification

Having prepared a suitable sample solution, especially in case of weakly scattering small solute particles, it is important to remove any components not wanted to contribute to the scattered intensity, such as dust particles or air bubbles. Air bubbles in principle could be removed by careful ultrasonication of the sample, but it is more recommended to degas the solvents used for sample preparation. Dust is removed either by filtration or, if this is not possible, by centrifugation. In addition, the light scattering cell itself has to be cleaned from dust. This can be done, for example, by repeatedly flushing it with filtered acetone and then leaving it to dry under a dust-free special hood. A better method is to clean the cuvettes and the cuvette Teflon lids (!) with refluxing and therefore guaranteed clean acetone for 15–30 min (using a home-built distillation column like the one described in the famous book on physical chemistry of macromolecules by Tanford [4.5]), and then leaving them to dry in a dust free hood. To avoid dust contamination during this step, the sample cuvettes should be placed upside-down while drying.

Next, the sample solution itself is filtered, if possible, into these clean and dry cuvettes, using a handheld syringe and a porous membrane filter cartridge attached to the outlet of the syringe. The material of the filter (Teflon, cellulose, etc.) has to be chosen according to the solvent used for the light scattering sample, the pore size (typically 0.2–0.45 μm) according to the size of the scattering particles. One of the best-known commercial providers for a variety of suitable filters is the company Millipore (see Chap. 6). Importantly, the concentration of the sample may be changed by the filtration process due to adsorption of solute particles onto the filter membrane. An indication of strong adsorption of the scattering particles to the filter membrane is clogging of the filter, which should be avoided either by switching to a different membrane type or to a larger pore

size up to 0.8 μm. To minimize the filtration losses in case of the absence of clogging, the filters have to be "conditioned" by filtering and discarding 1–2 mL of the sample solution before filling the light scattering cuvette. Still, filtration losses cannot be excluded after "conditioning" in every case. Whereas they play no role for dynamic light scattering experiments (see Table 4.1), it is crucial to detect them, and therefore accurately know the actual sample concentration, for static light scattering experiments. Here, the only possibility is to quantify the solute particle concentration before and after filtration, using, for example, uv/vis absorption spectroscopy. Only in case filtration does not work for a given sample, for example, due to serious filtration losses, centrifugation of dust particles onto the sample cuvette bottom and careful handling of the sample cell thereafter can provide a solution.

## References

4.1 Förster S, Schmidt M (1995) Polyelectrolytes in solution. Adv Polym Sci 120:51
4.2 Förster S, Hermsdorf N, Böttcher C, Lindner P (2002) Structure of polyelectrolyte copolymer micelles. Macromolecules 35:4096
4.3 Förster S, Schmidt M, Antonietti M (1990) Static and dynamic light scattering by aqueous polyelectrolyte solutions: Effect of molecular weight, charge density and added salt. Polymer 31:781
4.4 Vrij A, Overbeek, JTG (1962) Scattering of light by charged colloidal particles in salt solutions. J Colloid Interface Sci 17:570
4.5 Tanford, C (1961) Physical chemistry of macromolecules. Wiley, New York

# 5 Selected Examples of Light Scattering Experiments

In this chapter, I will try to illustrate the practice of experimental light scattering by several examples chosen from recent literature. As a starting point, let us first consider a general flow chart on how a light scattering experiment typically is planned depending on sample information already available and sample characterization desired (see Fig. 5.1).

Note that the scheme shown in Fig. 5.1 is valid only in case all samples studied are very dilute, and interparticle interactions for this reason can be neglected. Only then is the pure particle form factor detected in a static light scattering experiment, and the relaxation process measured in a dynamic light scattering experiment corresponds to the selfdiffusion coefficient defined by the Stokes–Einstein–equation (Eq. 1.47). Particularly the effect of interparticle interactions on the experimental results of a DLS measurement will be discussed in more detail further below (see Sect. 5.1).

Next, let us consider the case of an unknown sample topology in more detail, as described by the flow chart presented in Fig. 5.2.

Here, it should be noted that whereas $M_w$, $\langle R_g \rangle_z$, $A_2$ and $\langle R_H^{-1} \rangle_z$ can be accurately measured by light scattering for most samples, determination of the sample topology itself often is a very difficult task. This is most obvious for smaller particles <50 nm, where measurement of the particle form factor is beyond the length-scale resolution of the light scattering experiment and therefore only the $\rho$-ratio $R_g/R_H$ can provide an indication, but does not allow an unambiguous determination, of the particle shape. Also, in case of particles >50 nm, a large sample polydispersity may interfere with a detailed analysis of the particle form factor in a static light scattering experiment. Fractionation of the sample by GPC or FFF, and subsequent analysis of the less polydisperse sample fractions by light scattering in this case is the only way to achieve a reliable sample characterization, as already stated above.

The flow charts shown in Figs. 5.1 and 5.2 can only crudely summarize the experimental practice of light scattering. To illustrate the numerous applications of light scattering and also to provide detailed information on experimental procedure and data analysis of modern light scattering experiments, the author has tried to select a comprehensive set of representative examples from recent literature (1995 until now). All papers were written by widely accepted experts in

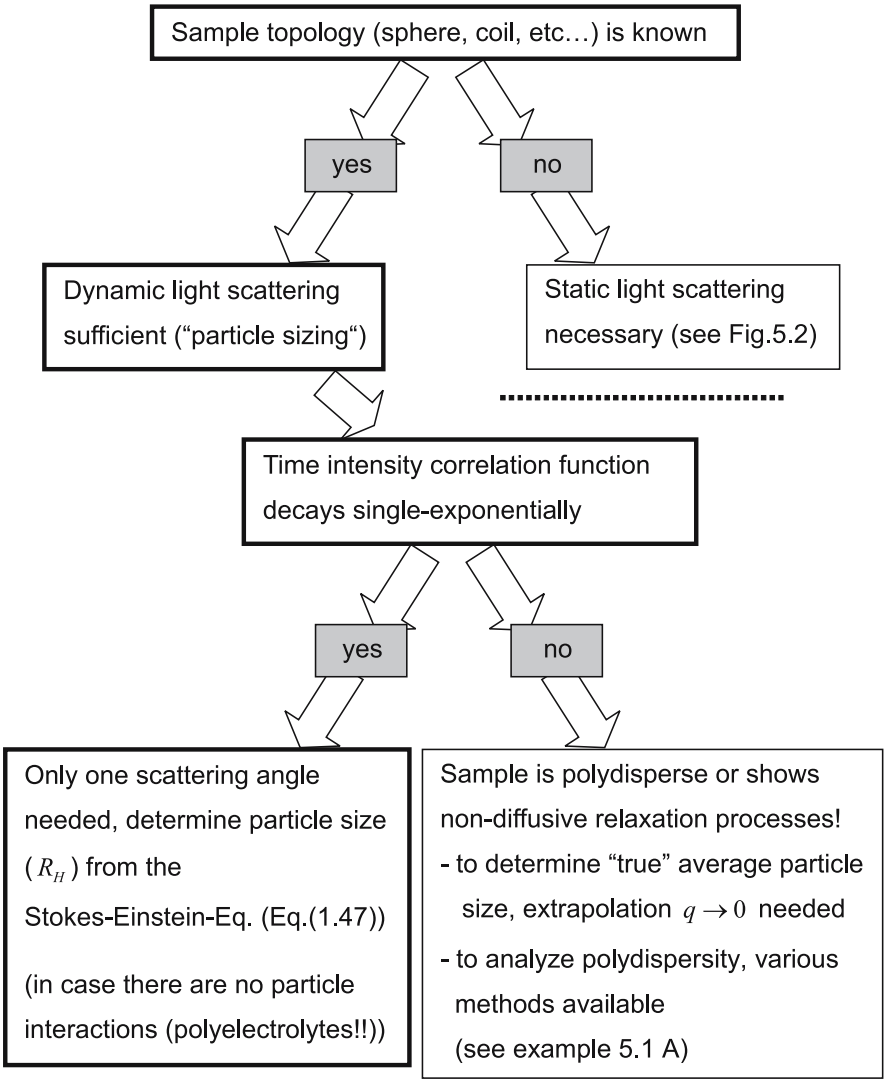


**Fig. 5.1**. Flow chart for sample characterization by laser light scattering – first part

the field of light scattering, and major contributors to the progress in application and experimental procedure of the light scattering method. We will now move on to a very important part of this book: a detailed review of examples from literature, presented in the context of the preceding chapters. All examples will be reviewed under the following aspects: (i) sample investigated and sample treatment before light scattering, (ii) light scattering setup used for the experiment, (iii) light scattering data and data analysis, (iv) concluding remarks.

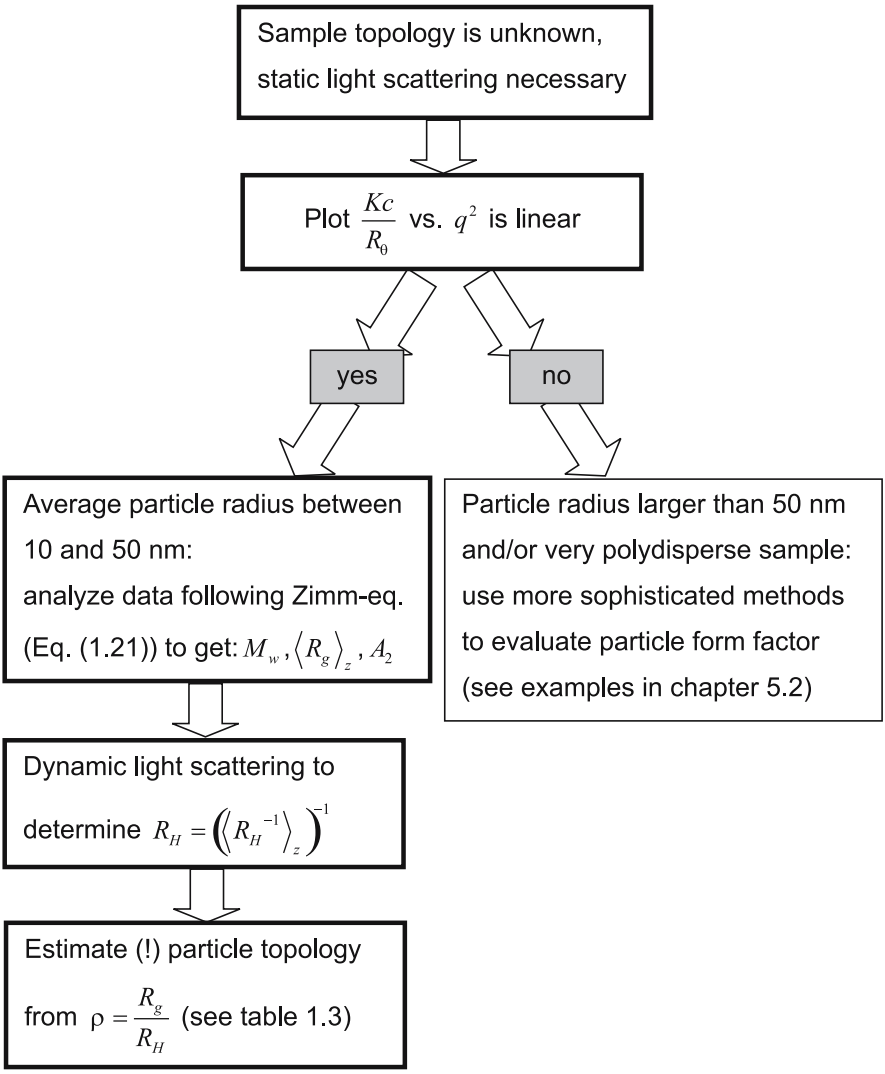


**Fig. 5.2**. Flow chart for sample characterization by laser light scattering – second part

In the first section of this chapter, several illustrative examples of the practice of pure dynamic light scattering studies are presented. One important aspect is the practice of polydispersity analysis. Another topic is the investigation of nonisotropic particles by dynamic light scattering. Also, the difficulties which may arise if solutions of charged scattering particles (= polyelectrolyte solutions) are investigated by dynamic light scattering are discussed.

In the second section, we will present several examples for light scattering studies of nanoscopic particles and polymer architectures of unknown topology. Here,

often a combination of static and dynamic light scattering is used to characterize the unknown particles, as shown in the flow charts (Figs. 5.1, 5.2). Additionally, a couple of different approaches concerning the data analysis of the static scattering intensity or particle form factor are presented, depending on average particle size in respect to the experimental length scale and particle topology.

Finally, in Sect. 5.3 I will present some experimental examples for the new experimental dynamic light scattering techniques described in Chap. 2 of this book: fiber optic quasi elastic light scattering (FOQELS), dual color dynamic light scattering, and dynamic light scattering using a CCD camera chip as area detector. Here, the application of DLS to the characterization of turbid samples, as well as an enhancement of the time-scale of the dynamic light scattering method will be illustrated.

## 5.1 Dynamic Light Scattering

In this section, I will first provide an experimental example for the practice of polydispersity data analysis in dynamic light scattering experiments, using a spherical latex dispersion as model sample. This first example will be followed by examples for DLS from branched polymer architectures and rod-like particles. DLS experiments from charged particles will be presented thereafter. Section 5.1 will conclude with examples from the literature that show the treatment of usually unwanted side effects encountered during a dynamic light scattering experiment, as aggregate formation, presence of dust, and absorption of the incident laser light.

**Example A (Ref. [2.1]):**
The authors of ref. [2.1], Vanhoudt and Clauwaert, were mainly interested in investigating the difference between fiber optic and pinhole detectors used in light scattering experiments. Importantly, their study also provides a very nice example for state-of-the art data analysis of DLS data from polydisperse samples, covering all methods currently in use. For their experiments, Vanhoudt and Clauwaert have chosen a well-defined binary mixture of commercially available standard latex particles. In briefly reviewing their results, we will restrict ourselves to the classical pinhole detector setup. This restriction is justified by the conclusions of the authors who claim that, besides a lower weight and therefore easier experimental handling, fiber optic detectors do not improve the size resolution of a dynamic light scattering experiment compared to conventional pinholes.

*(i) Samples and sample treatment:*
Aqueous dispersions of commercial latex beads 3020A and 3050A Nanosphere Size Standards from Duke Scientific Corp. and one standard from Balzers Co.